Differential response of injured and healthy retinas to syngeneic and allogeneic transplantation of a clonal cell line of immortalized olfactory ensheathing glia: a double-edged sword

María Norte-Muñoz[1], María Portela-Lomba[2,†], Paloma Sobrado-Calvo[1], Diana Simón[2], Johnny Di Pierdomenico[1], Alejandro Gallego-Ortega[1], Mar Pérez[3], José M. Cabrera-Maqueda[1,4], Javier Sierra[5], Manuel Vidal-Sanz[1], María Teresa Moreno-Flores[3,*], Marta Agudo-Barriuso[1,*]

https://doi.org/10.4103/NRR.NRR-D-23-01631

Date of submission: September 28, 2023

Date of decision: December 1, 2023

Date of acceptance: April 19, 2024

Date of web publication: May 13, 2024

From the Contents

Graphical Abstract

Effects of transplanting immortalized olfactory ensheathing glia into healthy or injured retinas

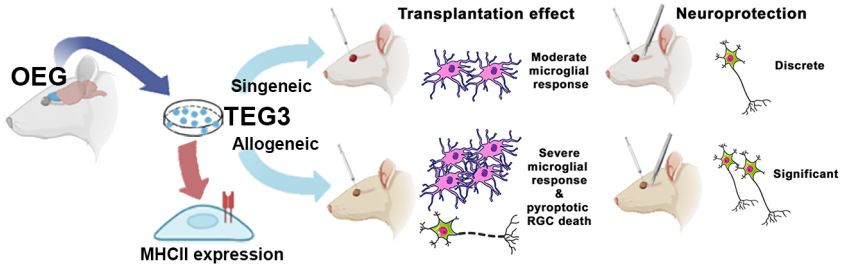

Abstract

Olfactory ensheathing glia promote axonal regeneration in the mammalian central nervous system, including retinal ganglion cell axonal growth through the injured optic nerve. Still, it is unknown whether olfactory ensheathing glia also have neuroprotective properties. Olfactory ensheathing glia express brain-derived neurotrophic factor, one of the best neuroprotectants for axotomized retinal ganglion cells. Therefore, we aimed to investigate the neuroprotective capacity of olfactory ensheating glia after optic nerve crush. Olfactory ensheathing glia cells from an established rat immortalized clonal cell line, TEG3, were intravitreally injected in intact and axotomized retinas in syngeneic and allogeneic mode with or without microglial inhibition or immunosuppressive treatments. Anatomical and gene expression analyses were performed. Olfactory bulb-derived primary olfactory ensheathing glia and TEG3 express major histocompatibility complex class II molecules. Allogeneically and syngenically transplanted TEG3 cells survived in the vitreous for up to 21 days, forming an epimembrane. In axotomized retinas, only the allogeneic TEG3 transplant rescued retinal ganglion cells at 7 days but not at 21 days. In these retinas, microglial anatomical activation was higher than after optic nerve crush alone. In intact retinas, both transplants activated microglial cells and caused retinal ganglion cell death at 21 days, a loss that was higher after allotransplantation, triggered by pyroptosis and partially rescued by microglial inhibition or immunosuppression. However, neuroprotection of axotomized retinal ganglion cells did not improve with these treatments. The different neuroprotective properties, different toxic effects, and different responses to microglial inhibitory treatments of olfactory ensheathing glia in the retina depending on the type of transplant highlight the importance of thorough preclinical studies to explore these variables.

Key Words: cell therapy; immune recognition; major histocompatibility complex class II (MHCII); neuroprotection; olfactory ensheathing glia; retinal ganglion cells

[1]Grupo de Investigación Oftalmología Experimental, Departamento de Oftalmología, Optometría, Otorrinolaringología y Anatomía Patológica, Facultad de Medicina, Universidad de Murcia, Instituto Murciano de Investigación Biosanitaria (IMIB), Campus de Ciencias de la Salud, Murcia, Spain; [2]Experimental Sciences Faculty, Universidad Francisco de Vitoria, Pozuelo de Alarcón, Madrid, Spain; [3]Anatomy, Histology and Neuroscience Department, Medicine Faculty, Universidad Autónoma de Madrid, Madrid, Spain; [4]Center of Neuroimmunology, Service of Neurology, Laboratory of Advanced Imaging in Neuroimmunological Diseases, Hospital Clínic of Barcelona, Institut d'Investigacions Biomèdiques August Pi i Sunyer (IDIBAPS), and Universitat de Barcelona, Barcelona, Spain; [5]Medicine Faculty, Universidad Francisco de Vitoria, Pozuelo de Alarcón, Madrid, Spain

†Current address: María Portela-Lomba, Department of Genetics and Development, Columbia University Medical Center, New York, NY, USA

***Correspondence to:** María Teresa Moreno-Flores, PhD, mteresa.moreno@uam.es; Marta Agudo-Barriuso, PhD, martabar@um.es.

https://orcid.org/0000-0002-8494-8143 (María Teresa Moreno-Flores); https://orcid.org/0000-0002-8566-9277 (Marta Agudo-Barriuso)

Funding: *This study was supported by the Spanish Ministry of Economy and Competitiveness, No. PID2019-106498GB-I00 (to MVS); the Instituto de Salud Carlos III, Fondo Europeo de Desarrollo Regional "Una manera de hacer Europa", No. PI19/00071 (to MAB); Ministerio de Ciencia e Innovación Project, No. SAF2017-82736-C2-1-R (to MTMF) in Universidad Autónoma de Madrid; and Fundación Universidad Francisco de Vitoria (to JS).*

How to cite this article: *Norte-Muñoz M, Portela-Lomba M, Sobrado-Calvo P, Simón D, Di Pierdomenico J, Gallego-Ortega A, Pérez M, Cabrera-Maqueda JM, Sierra J, Vidal-Sanz M, Moreno-Flores MT, Agudo-Barriuso M (2025) Differential response of injured and healthy retinas to syngeneic and allogeneic transplantation of a clonal cell line of immortalized olfactory ensheathing glia: a double-edged sword. Neural Regen Res 20(8):2395-2407.*

Introduction

Since Cajal's pioneering studies, it has long been clear that neurons from the central nervous system (CNS) regenerate poorly, in contrast to those from the peripheral nervous system (Cajal et al., 1991). Several strategies have been used to promote neuroprotection and CNS regeneration, including blocking or removing axonal growth inhibitors from myelin or the glial scar and cell transplantation approaches (Okano, 2002; Agudo et al., 2008; Bunge, 2016; Assinck et al., 2017; Lindsay et al., 2017; Gómez et al., 2018; Bradbury and Burnside, 2019).

A successful strategy has consisted of the use of olfactory ensheathing glia (OEG) due to their properties. OEG is located in the mammalian olfactory system and provides a pro-regenerative environment for olfactory sensory neuronal axons during the adult lifetime (Gómez et al., 2018). Olfactory sensory neurons are constantly renewed and OEG cells facilitate their axonal growth from the neuroepithelium to their targets in the olfactory bulb—mitral and tufted cells (Roet and Verhaagen, 2014; Gómez et al., 2018). The neuroregenerative capacity of primary cultured OEG and immortalized lines derived from these have been tested in an *in vitro* model of axotomized rat retinal ganglion cells (RGCs): OEG olfactory bulb and mucosa-derived but not lung or skin fibroblasts mediate *in vitro* axonal regeneration of RGCs (Moreno-Flores et al., 2003; García-Escudero et al., 2012; Portela-Lomba et al., 2020). The neuroregenerative capacity of OEG has also been assessed *in vivo* in rat models of spinal cord injury (Moreno-Flores et al., 2006; Khankan et al., 2016) and its reparative ability is due to a combination of neurotrophic and neuroprotective factors (Gómez et al., 2018). Clonal cell lines of immortalized rat and human OEG have been demonstrated to promote RGCs axonal regeneration in coculture, some of them as efficiently as primary OEG derived from the OB (Moreno-Flores et al., 2003, 2006; Lim et al., 2010). Moreover, TEG3, the most effective of the rat OEG immortalized clonal cell lines, was able to promote axonal repair in the dorsal columns of the rat-injured spinal cord, mediating functional recovery (Moreno-Flores et al., 2006).

In the visual system, peripheral nerve graft and other models of injury and regeneration of the optic nerve have demonstrated the possibility of obtaining axonal regeneration under determined experimental conditions (Bray et al., 1987; Vidal-Sanz et al., 2002). Using *in vivo* models, OEGs have been demonstrated to promote axonal regeneration of axotomized adult rat optic nerve axons (Li et al., 2003). Furthermore, OEG can rescue optic nerve axons in a model of glaucoma (Dai et al., 2019, 2012).

Intravitreal delivery of brain derived neurotrophic factor (BDNF) is the best neuroprotectant to date for axotomized RGCs induced by either complete optic nerve transection or crush (Peinado-Ramón et al., 1996; Parrilla-Reverter et al., 2009; Sánchez-Migallón et al., 2011). As primary OEG in culture, TEG3 cells express and secrete BDNF, contributing to the axonal regeneration of RGCs in coculture (Pastrana et al., 2006, 2007). Given these properties, we wondered whether OEG hold neuroprotective properties for axotomized RGCs.

Thus, here we tested OEG neuroprotective potential on axotomized RGCs using the established optic nerve crush (ONC) model (Nadal-Nicolás et al., 2009, 2015). We focused on allogeneic transplant alone or with immunosuppression because it is the most plausible treatment in the clinic and compare it with the syngeneic transplant. We analyzed the effect of both transplants on RGC survival and microglial activation after ONC, in intact retinas, as a control of a possible immune rejection to intravitreally transplanted cells (Norte-Muñoz et al., 2021, 2022). We also assessed the effect of microglial inhibition and systemic immunosuppression in both models and transplants. Finally, we studied the regulation of growth factors, gliosis, and pro- and anti-inflammatory mediators in intact and axotomized retinas after TEG3 allogeneic transplant with or without immunosuppression, and the death pathways activated in the transplanted intact retinas.

Methods

Animal handling

All animal procedures were approved by the Institutional Animal Care and Use Committee at the University of Murcia (Murcia, Spain) (approved protocols A13210201 and A1320140704) and performed according to the guidelines of our Institution, the 2010/63/EU directive on the protection of animals used for scientific purposes, and reported in accordance with the Animal Research: Reporting of *In Vivo* Experiments (ARRIVE) guidelines (Percie du Sert et al., 2020).

Adult female rats (Sprague–Dawley (allogeneic mode) and Wistar strains (syngeneic mode) used for allogeneic and syngeneic transplants) were obtained from the breeding colony of the University of Murcia or purchased from Envigo (Barcelona, Spain). Only females were used because they are smaller, less aggressive, and therefore easier to handle than males. Animals were kept at the University of Murcia animal housing facilities in temperature and light-controlled rooms (12-hour light/dark cycles) with food and water administered ad libitum.

Surgery and intravitreal injections were carried out under general anesthesia and administered intraperitoneally with a mixture of ketamine (60 mg/kg, Ketolar, Parke-Davies, S.L., Barcelona, Spain) and xylazine (10 mg/kg, Rompún, Bayer S.A., Barcelona, Spain). Analgesia was provided by subcutaneous administration of buprenorphine (0.1 mg/kg; Buprex, Buprenorphine 0.3 mg/mL; Schering-Plough, Madrid, Spain). During and after anesthesia, eyes were covered with an ointment (Tobrex; Alcon S.A., Barcelona, Spain) to prevent corneal desiccation. Animals were sacrificed with an intraperitoneal injection of an overdose of sodium pentobarbital (Dolethal, Vetoquinol; Especialidades Veterinarias, S.A., Alcobendas, Madrid, Spain).

Minocycline treatment was performed by daily intraperitoneal injections (45 mg/kg; M9511; Sigma, Darmstadt, Germany) as it was described previously (Di Pierdomenico et al., 2018). Immunosuppressive treatment started 1 day before the procedures and continued until sacrifice. Immunosuppression was carried out following approved protocol by University of Murcia (A13210201) that combines intraperitoneal daily

dexamethasone injection (1.6 mg/kg; Cortexonavet 2 mg/mL; Syva, León, Spain) and oral cyclosporine (210 mg/L; Cyclavance® 100 mg/mL; Virbac, Barcelona, Spain) diluted in water, as described (Norte-Muñoz et al., 2022).

Experimental design

Animals were randomly allocated to each experimental group (**Figure 1**), and none were excluded from the study. Confounders such as animal cages or treatment orders were not controlled. The authors MNM and MAB oversaw group allocation. **Figure 1** graphically summarizes the experimental groups, analyses, and corresponding figures in results. Controls were retinas from intact animals or matched non-TEG-3-transplanted groups. In intact animals, both retinas were analyzed. In the experimental animals that underwent intravitreal administration and/or ONC, only the left retina (treated and/or injured) was analyzed. The number of retinas per analysis and time point ranged from 3 to 6 and is detailed in the figure legends. The sample size was determined based on our experience with this model, where we would expect approximately 50% RGC loss at 7 days post-ONC, we used a non-parametric *t*-test which resulted in 3–6 animals per group to obtain consistent results to achieve statistical significance ($P < 0.05$) while adhering to the 3Rs (Charan and Kantharia, 2013).

Rat primary olfactory ensheathing glia and TEG3 *in vitro* culture

OEG cultures were carried out at the Tissue Culture Facilities (ACTI, University of Murcia and IMIB-Pascual Parrilla; and Universidad Francisco de Vitoria Laboratories).

Rat olfactory ensheathing glia primary culture

OEG from p21 RccHan®: WIST rat olfactory bulbs (OEG-ROB) were dissected, as follows: meninges were removed, and the external OB layer was separated and cut with a scalpel blade to obtain pieces < 1 mm. These were placed in a 15 mL Falcon and centrifuged at 200 × *g*, 5 minutes. Then 2 mL of 0.1% trypsin was added to the pellet and incubated for 15 minutes at 37°C with intermittent shaking. To stop trypsin digestion 4 mL of $HBSS^{+}$ were added (HBSS supplemented with 20 % fetal bovine serum (FBS; Gibco) and 2000 U/mL DNAse), and the suspension was centrifuged at 200 × *g* for 5 minutes. The pellet was resuspended in 2 mL of $HBSS^{+}$ and it was mechanically disaggregated by pipetting 20 times with glass Pasteur pipets of different caliber. Tissue suspension was centrifuged at 200 × *g* for 10 minutes, and cells were resuspended in 3 mL of ME medium (composed of DMEM/F12 (Gibco, Cat# 11320074) supplemented with 10% FBS (GE Healthcare Hyclone), 2 mM glutamine (Gibco, Cat# 25030024), 20 µg/mL pituitary extract (Gibco, Cat# 13028014), 2 µM

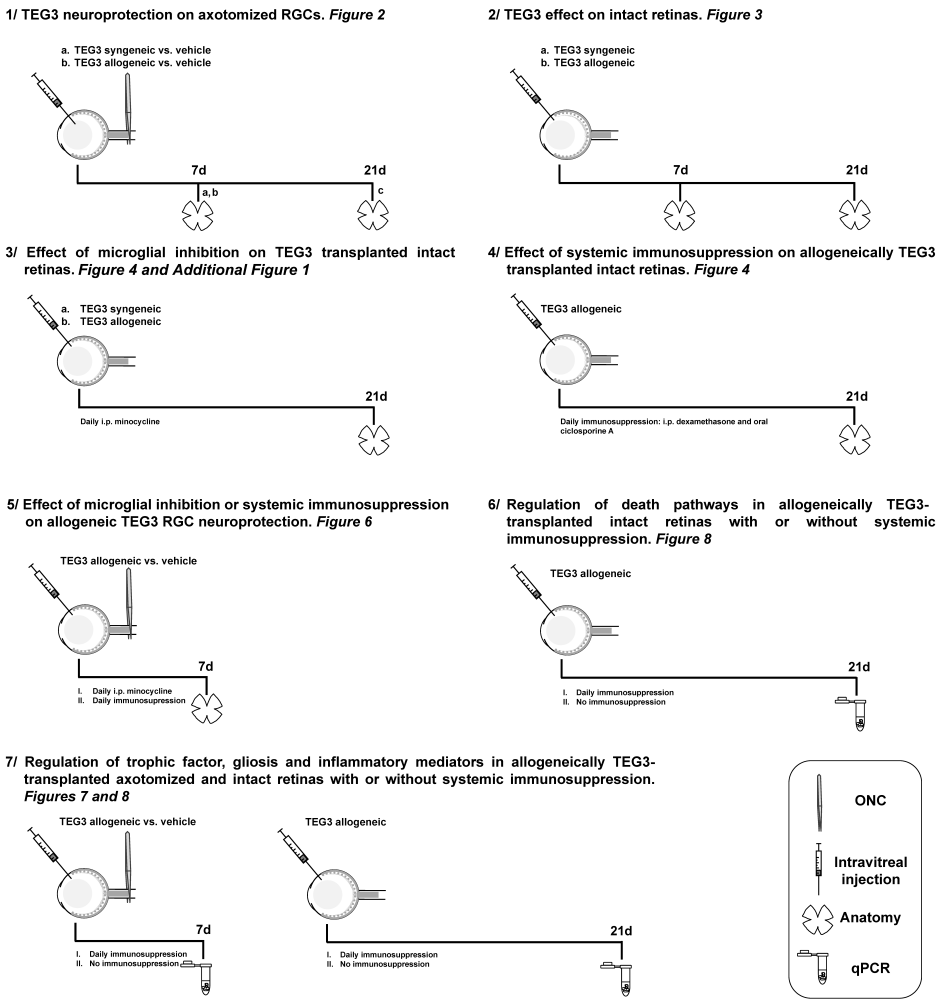

Figure 1 | **Experimental design.** Experimental groups and analyses. Controls for anatomy: intact retinas. For ONC + TEG3 transplantation: vehicle. For minocycline or immunosuppression treated groups (3–5): group 1 for group 5, and group 2 for groups 3 and 4. *n* = 3–6 retinas/time point/analyses. ONC: Optic nerve crush; qPCR: quantitative polymerase chain reaction; RGCs: retinal ganglion cells; TEG3: OEG immortalized clonal cell line.

forskolin (Sigma, Cat# F6886) and an antibiotic and antifungal solution (Pen/Strep/Fung 10,000 IU/10,000 IU/25 µg, Lonza, Cat# 17-745E) and distributed in three p60 culture plates (1 mL per p60; Falcon), pre-treated with poly-L-lysine (PLL, 10 µg/mL; Sigma). ROB cells were maintained a 37°C, 5% CO_2 The culture medium was changed twice per week until confluence was reached.

Rat TEG3 culture

Immortalized OEG clonal cell line TEG3 is an SV40 large T antigen stable transfectant of OEG primary cultures prepared from adult Wistar rat olfactory bulbs. These cells were cultured and expanded as previously described (Moreno-Flores et al., 2003). TEG3 cells used *in vivo* were transduced to stably express green fluorescent protein (GFP). Briefly, cells were seeded in a 60 mm culture dish (Cultek, Madrid, Spain, Cat# 45353002) and maintained in ME medium at 37°C and 5% CO_2 up to ~80% confluence when cells were prepared for intravitreal injection in Dulbecco's Modified Eagle Medium (DMEM). We used non-GFP transduced cells for immunodetection of type II molecules of the rat major histocompatibility complex class II (MHCII) in cultured non-confluent TEG3 cells.

Optic nerve crush

The left optic nerve was crushed following previously described methods (Parrilla-Reverter et al., 2009). Briefly, to access the optic nerve at the back of the eye, an incision was made in the skin overlying the superior orbital rim, the supero-external orbital contents were dissected, and the superior and external rectus muscles were sectioned. Then, the optic nerve was crushed at 0.5 mm from the optic disc for 10 seconds using watchmaker's forceps (Fine Science Tools, Heidelberg, Germany). Before and after the procedure, the eye fundus was observed through the operating microscope to assess the integrity of the retinal blood flow.

Intravitreal injections

In intact retinas or immediately after ONC, GFP^+ TEG3 cells were administered in DMEM medium at a concentration of 16×10^3 cells/µL in 5 µL final volume following published methods (Peinado-Ramón et al., 1996; Parrilla-Reverter et al., 2009). Vehicle animals were injected with 5 µL of DMEM. In all groups, intravitreal injections were done in the left eye.

Quantitative reverse transcription-polymerase chain reaction

Axotomized (groups: vehicle or TEG3, with or without immunosuppression) and intact (groups: TEG3 with or without immunosuppression) retinas were freshly dissected 7 days after ONC or 21 days after TEG3 transplant, respectively, and immediately submerged in NucleoZOL (Macherey-Nagel GmbH & Co. KG, Dueren, Germany, Cat# 740404.200). Total RNA was extracted following manufactured instructions and samples were dissolved in 20 µL Milli-Q water. Total RNA concentration was determined using SimpliNano (GE Healthcare Life Sciences, Madrid, Spain). Total RNA (1 µg) was used for complementary DNA amplification according to the instructions of the High-Capacity cDNA Reverse Transcription Kit (Thermo Fisher Scientific, Cat# 4368814).

SYBR Premix Ex Taq II (Tli RNaseH Plus, TaKara; Thermo Fisher Scientific)-based quantitative reverse transcription-polymerase chain reaction (qRT-PCR) was carried out by the Genomic Platform at the IMIB-Pascual Parrilla in a final volume of 5 µL with a primer concentration of 450 nM using the QuantStudio 5 (Applied Biosystems; Thermo Fisher Scientific). The qRT-PCR conditions were: 95°C for 30 seconds of denaturation, followed by 40 cycles of 95°C for 15 seconds, and 60°C for 60 seconds. Technical triplicates were done for each sample.

Rat SYBR green pre-designed primers were purchased from Sigma for the following genes: *Bdnf*, *Gfap*, *Il1β*, *Il6*, *Ptprc*, *Tnf*, *Il10*, *Tgfβ3*, *Cxcr2*, *Tgrfβ1*, *Cxcl5*, *Casp4*, *Casp3*, *Casp8*, *Gsdmd*, *Tnfrsf1a*, *Ctsb* (Cat# R-Bdnf-1, R-Gfap-1, R-Il1b-1, R-Il6-1, R-Ptprc-1, R-Tnf-1, R-Il10-1, R-Tgfb3-1, R-Cxcr2-1, R-Tgrfb1-1, R-Cxcl5-1, R-Casp4-1, R-Casp3-1, R-Casp8-1, R-Gsdmd-1, R-Tnfrsf1a-1, R-Ctsb-1). Three candidate reference genes (*Hprt*, *Rpl13a*, and *Actb*; Cat# R-Hprt-1, R-Rpl13a-1, and R-Actb-1) were evaluated and the most thermostable was *Hprt*, and thus it was used as reference gene. The Ct values were converted to fold change *versus* intact using the $2^{\Delta\Delta Ct}$ method (Livak and Schmittgen, 2001).

Cell and tissue processing and immunodetection

Animals were perfused transcardially with 0.9% saline solution followed by 4% paraformaldehyde in 0.1 M phosphate buffer. Retinal dissection and flat-mounted preparation were performed as previously described (Nadal-Nicolás et al., 2009).

Retinas were immunodetected with mouse anti-Brn3a (1:500; Millipore, Madrid, Spain, Cat# MAB1585, RRID: AB_94166) to quantify the total number of RGCs and rabbit anti-ionized calcium-binding adapter molecule 1 (Iba1; 1:500; Abcam, Cambridge, UK, ab178846, RRID: AB_2636859) to study microglial morphology. TEG3 cells were identified by their GFP expression.

Immunodetection on retinal whole mounts was performed as previously described (Nadal-Nicolás et al., 2009). Briefly, the retinas were permeabilized in phosphate-buffered saline (PBS) with 0.5% Triton by freezing them for 15 minutes at –70°C, rinsed in new PBS 0.5% Triton, and incubated overnight at 4°C with the primary antibodies diluted in blocking buffer (PBS, 2% normal donkey serum, 2% Triton). Then, the retinas were washed three times in PBS and incubated for 2 hours at room temperature with the secondary antibody diluted 1:500 in PBS-2% Triton. Finally, they were thoroughly washed in PBS and mounted vitreous side up on subbed slides.

Cultured TEG3 and ROB cells (rat olfactory bulb primary OEG) were plated in coverslips, fixed with 4% paraformaldehyde in PBS and immunolabeled to detect the MHC of rat (RT1), specifically rat MHCII B molecules (RT1.B) with mouse anti-MHCII RT1B, clone OX-6 (1:50; Bio-Rad, Madrid, Spain, Cat# MCA46R, RRID: AB_322404). Secondary detection was carried out with Alexa Fluor-labelled secondary antibody (1:500; Molecular Probes; Thermo Fisher Scientific) .

Retinal whole-mounts were mounted with anti-fading mounting media, and cross sections with the same medium containing 4'6-diamidino-2-phenylindole (DAPI; H-1200,

Vectashield®, Vector Laboratories Inc., Burlingame, CA, USA) to counterstain all cell nuclei. After immunodetection in TEG3 and ROB cells the samples were incubated for 5 minutes with DAPI (1 µg/mL, Merck, Madrid, Spain, Cat# D8417) and finally mounted with Fluoromount (Merck, Cat# F4680).

Image acquisition and analyses

Individual squared images of 500 μm^2 were acquired using a Leica DM6B epifluorescence microscope (Leica, Wetzlar, Germany). $Brn3a^+$ RGCs were quantified automatically and retinal photomontages were reconstructed from those images as previously reported (Nadal-Nicolas et al., 2009; Sánchez-Migallon et al., 2011; Norte-Muñoz et al., 2021, 2022). Briefly, the process involved initial steps of background intensity reduction using the Flatten filter and impulse noise removal with the Median filter. Subsequent image conversion to 16-bit grayscale and application of the $Edge^+$ spectral filter enhanced positive cell visibility. To address cell cluster separation, a dual-pass IPP watershed split morphologic filter was utilized, eroding and dilating objects to effectively isolate overlapping clusters. Nuclei were then counted based on predetermined size parameters, excluding objects beyond the scope of RGC nuclei. The final step involved displaying and exporting count data through an excell data sheet. RGC topographical distribution was assessed by isodensity maps using previously reported methods (Nadal-Nicolás et al., 2009). Isodensity maps show the density of RGCs with a color scale that goes from 0–500 RGCs/mm^2 (purple) to ≥ 3200 RGCs/mm^2 (red).

A Leica TCS SP5 spectral confocal microscope and LAS-AF software were used for confocal image acquisition. Images were taken with a 40× objective and using 405 nm (DAPI staining) and 488 nm (green MHCII immunostaining) laser lines.

Statistical analyses

This study was not blinded as the experimental animals and OEG-transplanted retinas were easily identifiable. All data were analyzed by non-parametric Mann–Whitney *U* test and plotted with GraphPad Prism v.7 (GraphPad Software, San Diego, CA, USA). RGC survival was graphed as mean total number ± standard deviation (SD), and qRT-PCR data as fold change *versus* intact (value 1) ± standard error of the mean (SEM). Groups were compared with intact or vehicle within the same analyses. Differences were considered significant when $P < 0.05$.

Results

Intravitreal allogeneic but not syngeneic TEG3 transplantation neuroprotects axotomized retinal ganglion cells

First, we tested the neuroprotective potential of intravitreally injected TEG3 cells on axotomized RGCs. TEG3 cells come from Wistar rats and were injected into the vitreous of Wistar (syngeneic mode) or Sprague-Dawley (allogeneic mode) rats right after ONC. Retinas were anatomically analyzed 7 days later, when without treatment > 50% of RGCs have died (Nadal-Nicolás et al., 2015; Vidal-Sanz et al., 2017). We observed that only the allogeneic transplant elicited significant RGC neuroprotection (**Figure 2A–C**). We, therefore, investigated whether allogeneic TEG3 neuroprotection was still observed after 21 days when 85% of RGCs would have died without treatment. As shown in **Figure 2D**, there was no difference in the number of RGC between retinas treated either with TEG3 or vehicle. Therefore, TEG3 neuroprotection was transient.

Finally, we observed the morphological activation of microglia identified by Iba1 immunodetection. We found that in both syngeneic and allogeneic TEG3-transplanted retinas, microglial cells were more activated than after ONC alone, an activation that increased from 7 to 21 days (**Figure 2E** and **F**). In the retina, as in the rest of the central nervous system, Iba1 was specifically expressed by microglial cells (**Additional Figure 1A**). However, this protein was also expressed by peripheral macrophages. Although most of the $Iba1^+$ cells in the experimental retinas would be microglial cells, we could not exclude macrophage infiltration after TEG3 transplantation, which once infiltrated were indistinguishable from microglial cells.

The intravitreal graft of TEG3 in intact retinas activates microglial cells and causes retinal ganglion cell death

In view of the above results, we wondered whether TEG3 cells elicited an immune or toxic response in intact retinas. Allogeneic and syngeneic TEG3 were transplanted into intact animals, and retinas were analyzed 7 or 21 days later. At 7 days, both transplants induced microglial activation, which was more significant and pronounced in the allogeneic transplants and increased in both scenarios at 21 days (**Figure 3A**). We then analyzed the RGCs, and to our surprise, both transplants caused significant RGC death after 21 days, which was greater with the allogeneic transplant (**Figure 3B–D**), despite being this transplant neuroprotectant to axotomized RGCs.

In vivo 21 days after transplantation into intact retinas, GFP^+ TEG3 cells were still present in the vitreous, forming an epimembrane without integrating into the retina (**Figure 4A**). Here, we also described a fact that was probably fundamental to the transplantation effects of OEG: in culture, TEG3 cells, like other OEG cells from olfactory bulb tested – i.e., primary cultured ROB cells – immunostained for MHCII (**Figure 4B**). Therefore, to our knowledge, OEGs have been unveiled as antigen-presenting cells for the first time. Possible implications of our finding for TEG3 transplantation in our retina experimental paradigms are discussed.

Microglial inhibition with minocycline or systemic immunosuppression rescues retinal ganglion cells from TEG3 toxicity in intact retinas but does not improve neuroprotection by allogeneic TEG3 transplantation

Microglial cells in the transplanted retinas were highly activated and we thought that this activation may play a role in RGC death through an uncontrolled inflammatory response. Thus, the next group of intact animals treated with intravitreal TEG3 or vehicle was systemically treated with minocycline. This tetracycline antibiotic selectively inhibits microglial cells (Kobayashi et al., 2013) and was analyzed at 21 days, when we observed that the TEG3 transplants caused RGC loss. In the syngeneic transplant, microglial inhibition did not rescue

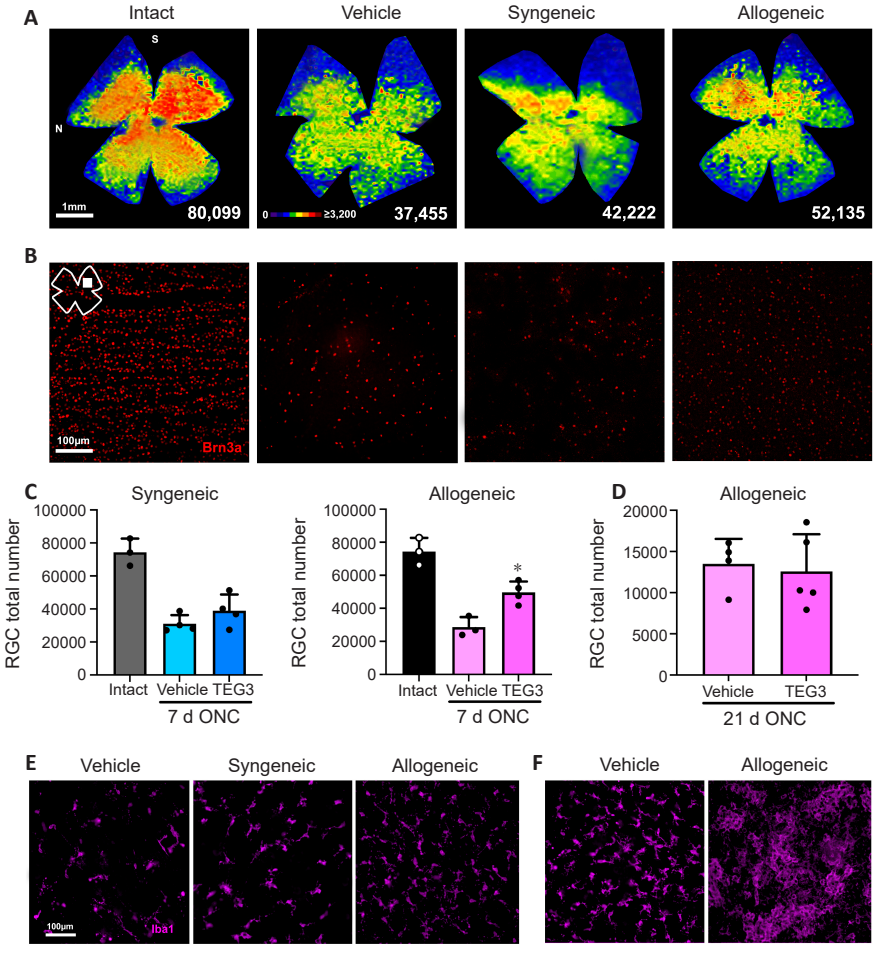

Figure 2 | Allogeneic transplant of TEG3 rescues axotomized RGCs but activates microglial cells.

(A) Isodensity maps showing the distribution of RGCs in intact retinas and retinas analyzed 7 days after ONC and vehicle, syngeneic, or allogeneic TEG3 intravitreal administration. Color coded density scale in the vehicle map goes from purple (0–500 RGCs/mm^2) to red (≥ 3200 RGCs/mm^2). Below each map is shown the number of RGCs counted in that retina. (B) Magnifications from flat-mounted retinas showing Brn3a$^+$ RGCs in each group. Images were taken from the middle retina (square in the retinal drawing). (C) Column bar graphs showing the mean total number of RGCs ± SD in the same groups as above. *P < 0.05, *vs.* vehicle (non-parametric Mann-Whitney *U* test). n = 3–5 retinas/group. (D) Column bar graphs showing the mean total number of RGCs ± SD in retinas analyzed 21 days after ONC and allogeneic TEG3 intravitreal administration. (E) Magnifications from retinal flat mounts showing Iba1$^+$ immunodetected microglial cells (purple) in retinas analyzed 7 days after ONC and vehicle, and ONC and syngeneic or allogeneic TEG3 intravitreal administration. The vehicle image is from an SD rat since there are no differences between rat strains to ONC. (F) Magnifications from retinal flat mounts showing Iba1$^+$ immunodetected microglial cells (purple) in retinas analyzed 21 days after ONC and vehicle or allogeneic TEG3 intravitreal administration. N: Nasal pole; ONC: optic nerve crush; RGCs: retinal ganglion cells; S: superior pole; TEG3: OEG immortalized clonal cell line.

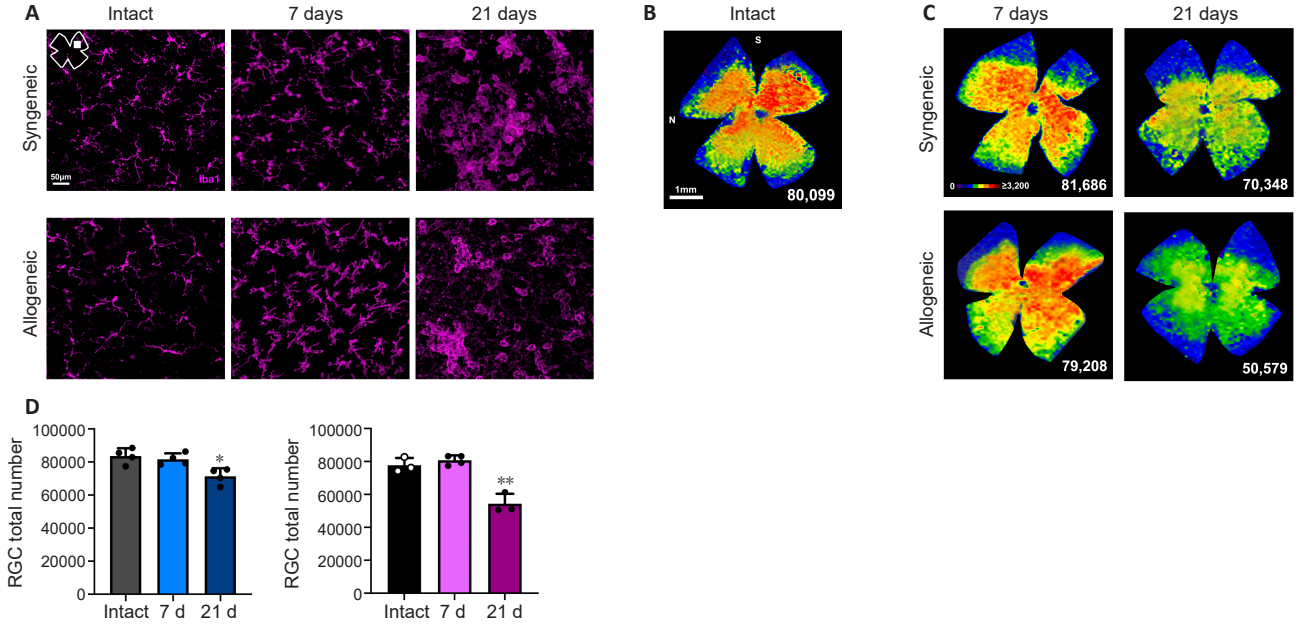

Figure 3 | The intravitreal graft of TEG3 in intact retinas causes RGC death and activates microglial cells.

(A) Magnifications from flat-mounted retinas showing Iba1$^+$ microglial cells (purple) in intact retinas from Wistar and SD rats, and in the same strains 7 and 21 days after TEG3 syngeneic (Wistar) or allogeneic (SD) transplantation. Images were taken from the middle retina (square in the retinal drawing). (B, C) Isodensity maps showing the distribution of RGCs in intact (B) and transplanted retinas (C) analyzed at 7 or 21 days after syngeneic or allogeneic TEG3 intravitreal transplantation. The color-coded density scale in B goes from purple (0–500 RGCs/mm^2) to red (≥ 3200 RGCs/mm^2). Below, each map is shown the number of RGCs counted in that retina. (D) Column bar graphs showing the mean total number of RGCs ± SD in intact and transplanted retinas at both time points (left syngeneic transplant and right allogeneic transplant). Percentages show the proportion of RGC loss *vs*. intact retinas (100%). *P < 0.05, **P < 0.01, *vs*. intact (non-parametric Mann–Whitney *U* tests). n = 5 retinas/time point/group. N: Nasal pole; RGCs: retinal ganglion cells; S: superior pole; TEG3: OEG immortalized clonal cell line.

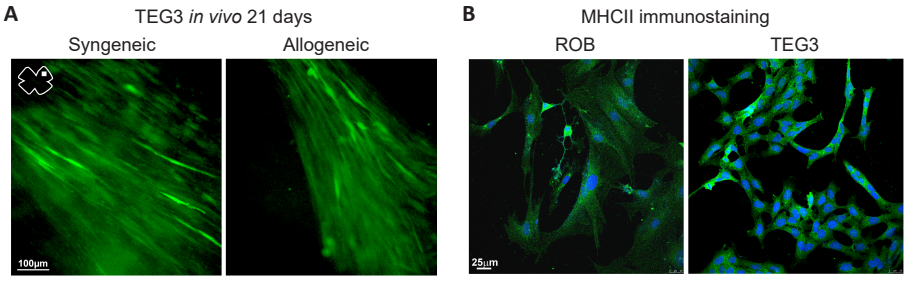

Figure 4 | TEG3 cells form an epimembrane after intravitreal administration without integrating into the retina and express MHCII constitutively.
(A) At 21 days after intravitreal syngeneic or allogeneic graft, TEG3 expressing green fluorescent protein (green) remains in the vitreous, forming an epimembrane on top of the retina. (B) Immunostaining for MHCII molecules (RT1.B) (green) in cultured rat primary OB-OEG cells - ROB line- and immortalized clonal cell line TEG3 cells. MHCII: Major histocompatibility complex class II; ROB cells: rat olfactory bulb primary OEGs; TEG3: OEG immortalized clonal cell line.

RGCs (**Additional Figure 1B** and **C**). However, in allogeneic transplantation, RGC loss decreased from 33% to 19% (**Figure 5A** and **B**), similar to the percentage of loss observed in syngeneic transplantation with or without minocycline treatment.

Microglial cells in TEG3$^+$ minocycline intact retinas showed a lower level of anatomical activation than in TEG3 intact retinas, in which microglia appeared more ameboid than after minocycline treatment (**Figures 5C** and **Additional Figure 1A**).

We then analyzed the effect of systemic immunosuppression on RGC survival 21 days after allogeneic TEG3 transplantation in intact retinas. We found that the rescue effect was no different from that observed with minocycline (**Figure 5A** and **B**). Microglial cells in TEG3 immunosuppressed intact retinas had a less activated morphology than in TEG3-intact retinas and a different morphology than in the minocycline group (**Figures 5C** and **Additional Figure 1A**).

Since both treatments rescued RGCs in allogeneic transplanted intact retinas, we investigated whether these treatments improved TEG3-induced RGC neuroprotection after ONC. Neither treatment synergized with TEG3 neuroprotection at 7 days. However, both systemic therapies were able to neuroprotect RGCs as well (minocycline) or better (immunosuppression) than TEG3 alone (**Figure 6A–C**).

Regulation of trophic factors, inflammatory, and death mediators in TEG3-transplanted retinas

Finally, we performed qRT-PCR on retinal extracts from axotomized groups (**Figure 7**) or intact (**Figure 8**) with or without allogeneic TEG3 and/or immunosuppression. Intact and axotomized retinas were analyzed at 21 and 7 days, respectively. We analyzed the regulation of Bdnf, a neuroprotective trophic factor for axotomized RGCs which is expressed by TEG3 *in vitro* (Pastrana et al., 2007, 2006), micro- and macroglial activation (*Ptprc*, *Gfap*) and inflammatory mediators (*Cxcr2*, *Il10*, *Tgfβ1*, *Tgfβ3*, *Cxcl5*, *Tnf*, *Il6*, and *Il1β*; **Figures 7** and **8**).

In the intact groups, we also observed key genes in different death pathways (pyroptosis: *Casp4*, *Gsdmd*; apoptosis: *Casp3*; extrinsic apoptosis: *Tnfrsf1a*, Intrinsic apoptosis: *Casp8*, *Ctsb*; **Figure 8**). This analysis was not performed on axotomized retinas because we wanted to isolate the effect of TEG3 transplantation on RGC death.

Compared with their respective controls, *Bdnf* was upregulated in ONC-TEG3 retinas and the immunosuppressive treatment significantly reduced this upregulation. Interestingly, in intact-TEG3 retinas, *Bdnf* was not upregulated, and immunosuppression reduced its levels but not significantly.

Expression of *Ptprc*, the gene encoding CD45, a marker of activated microglial cells and leukocytes, increased in TEG3-transplanted intact or axotomized retinas. In both cases, *Ptprc* expression was controlled by immunosuppression, in agreement with the anatomical data.

Gfap, a macroglial marker (astrocytes and Müller cells in the retina), was upregulated in ONC + TEG3 retinas. ONC alone or TEG3 transplant in intact retinas did not significantly increase *Gfap* expression, the former in accordance with previous anatomical data (González-Riquelme et al., 2021).

Interestingly, while immunosuppression decreased *Gfap* levels in injured TEG3 retinas, it did increase them significantly in intact + TEG3 retinas. When transplanted, this differential response to immunosuppression between intact or axotomized retinas was also observed for *Tfgb3*, *Cxcl5*, and *Cxcr2*.

TEG3 transplant increased the expression of proinflammatory molecules *Il1β* and *Tnf* in intact retinas and of *Tnf* in ONC retinas. Immunosuppression reverted this up-regulation in intact retinas but increased *Il1β* in ONC retinas.

Il6, a dual cytokine, was upregulated by TEG3 in ONC retinas, and again, this upregulation was controlled by immunosuppression.

Il10, an anti-inflammatory cytokine, increased in TEG3-treated retinas and after immunosuppression.

In intact retinas, the TEG3 transplant significantly increased the levels of *Casp4*, which is indicative of pyroptosis, which was not minimized by immunosuppression. However, immunosuppression also increased *Tnfrs1a* while downregulating its ligand *Tnf*.

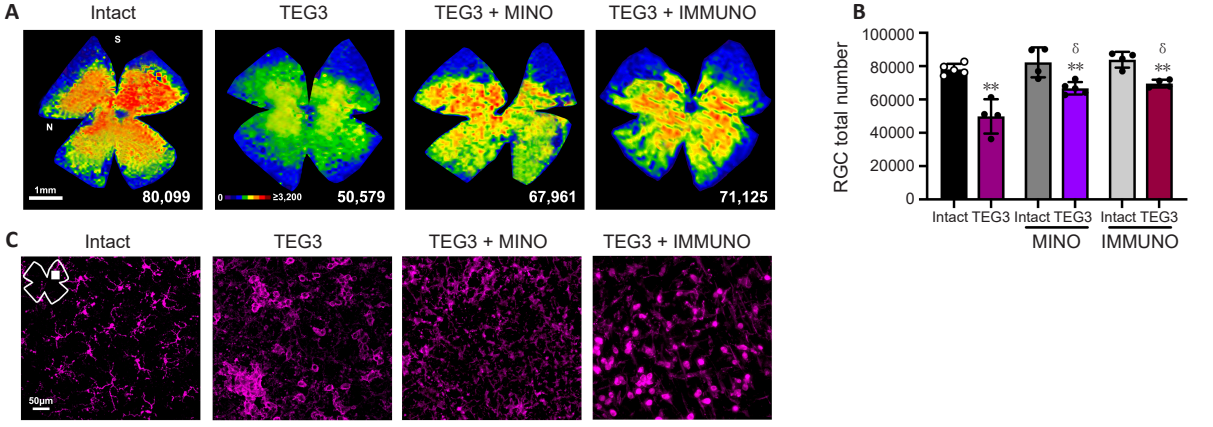

Figure 5 | Microglial inhibition with minocycline or systemic immunosuppression rescues RGCs from TEG3 toxicity in intact retinas.
(A) Isodensity maps showing the distribution of RGCs in intact retinas and intact retinas with allogeneic TEG3 transplant with or without systemic MINO or IMMUNO. Retinas were analyzed 21 days after the grafts. The coded density scale in the TEG3 map goes from purple (0–500 RGCs/mm^2) to red (≥ 3200 RGCs/mm^2). Below each map is shown the number of RGCs counted in that retina. (B) Column bar graphs showing the mean total number of RGCs ± SD in the same groups as above as well as non-grafted retinas treated with minocycline or immunosuppression. **P < 0.01, *vs*. their corresponding intact animals; δP < 0.05, *vs*. non-treated TEG3 group (non-parametric Mann–Whitney U test). n = 4–6 retinas/group. (C) Magnifications from flat-mounted retinas showing Iba1$^+$ microglial cells (purple) in intact retinas and intact retinas with allogeneic TEG3 graft with or without systemic MINO or IMMUNO. Images were taken from the middle retina (square in the retinal drawing). IMMUNO: Immunosuppression; MINO: minocycline; N: nasal pole; RGCs: retinal ganglion cells; S: superior pole; TEG3: OEG immortalized clonal cell line.

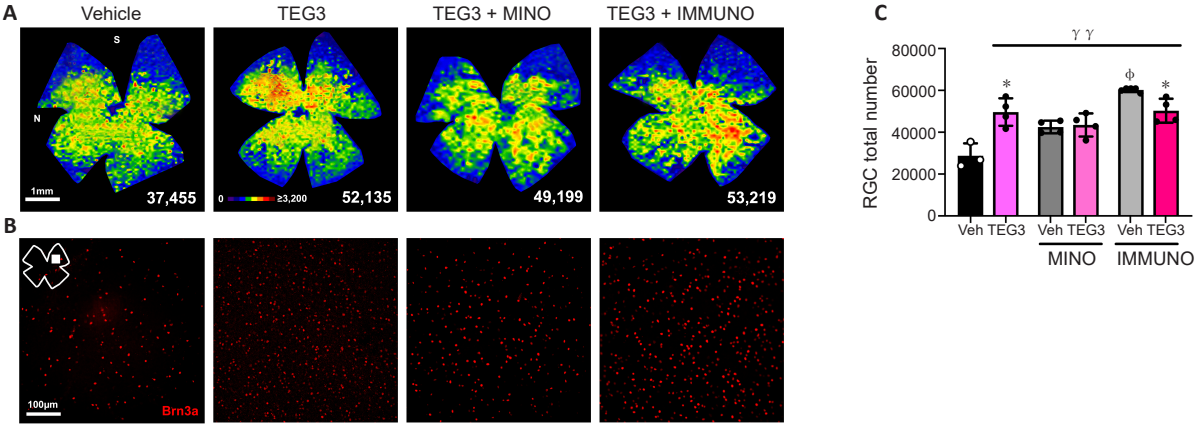

Figure 6 | Microglial inhibition with minocycline or systemic immunosuppression rescues RGCs but does not synergize with TEG3 neuroprotection.
(A) Isodensity maps showing the distribution of RGCs in axotomized retinas treated with vehicle or allogeneic TEG3 graft with or without systemic minocycline or immunosuppression. Retinas were analyzed 7 days after ONC. The color-coded density scale in the TEG3 map goes from purple (0–500 RGCs/mm^2) to red (≥ 3200 RGCs/mm^2). Below, each map is shown the number of RGCs counted in that retina. (B) Magnifications from flat-mounted retinas show Brn3a$^+$ RGCs in each group. Images were taken from the middle retina (square in the retinal drawing). (C) Column bar graphs showing the mean total number of RGCs ± SD in the above mentioned groups. *P < 0.05, *vs*. their corresponding vehicle; ϕP < 0.05, *vs*. vehicle without treatment (the first column in black); γγP < 0.01, all groups *vs*. vehicle without treatment (non-parametric Mann–Whitney U tests). n = 4–6 retinas/group. IMMUNO: Immunosuppression; MINO: minocycline; N: nasal pole; RGCs: retinal ganglion cells; S: superior pole; TEG3: OEG immortalized clonal cell line; Veh: vehicle.

Discussion

BDNF has been shown to have a neuroprotective role on RGCs after optic nerve axotomy (Peinado-Ramón et al., 1996; Martin and Quigley, 2004; Parrilla-Reverter et al., 2009; Sánchez-Migallón et al., 2011; Lambuk et al., 2022). In addition, BDNF secreted by TEG3 is essential for axonal regeneration of adult RGCs cocultured with TEG3 (Pastrana et al., 2006, 2007).

Therefore, we expected TEG3 to be neuroprotective for axotomized RGCs. Indeed, this was true for allogeneic transplants. Unexpectedly, although syngeneic transplantation also showed a positive shift towards RGC rescue, the effect was not significant. This was puzzling because we predicted a higher neuroprotection with the syngeneic transplant. We do not know why, but it is possible that TEG3 cells, as shown for MSC (Klinker et al., 2017), increase their immunomodulatory properties after an inflammatory challenge. As the immune response in syngeneic transplantation is lower than in allogeneic transplantation (Norte-Muñoz et al., 2022), it is possible that the inflammatory environment in the former does not sufficiently stimulate TEG3 cells to secrete high enough levels of neuroprotective factors.

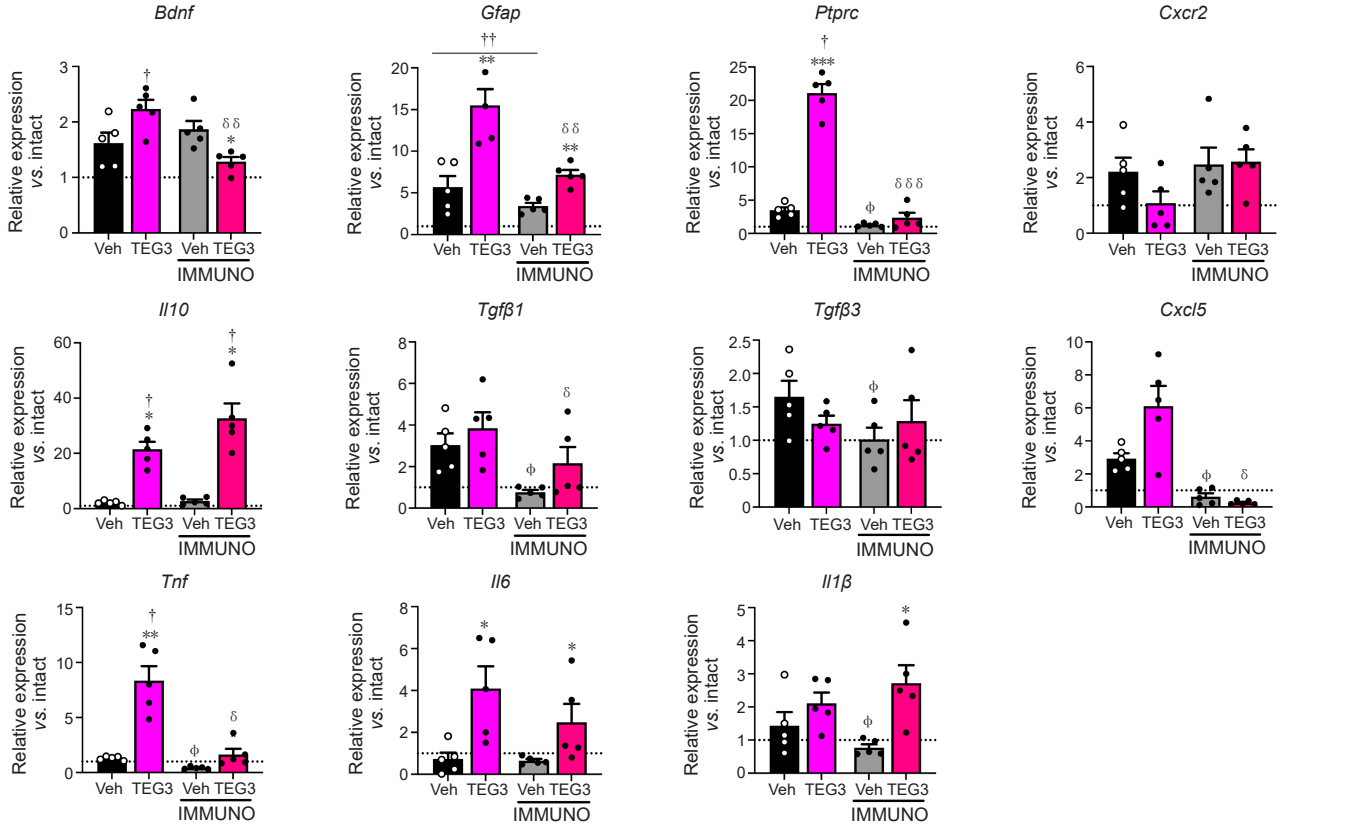

Figure 7 | **Effects of ONC, immunosuppression, and TEG3 transplantation on gene expression in the retina.**
Bar graphs showing gene expression levels 7 days after ONC in vehicle or TEG-3 allogeneically transplanted retinas with or without INMUNO compared with intact non-immunosuppressed retinas (value 1, horizontal dashed line). *Bdnf*: Neuroprotective trophic factor; *Cxcr2*, *Il10*, *Tgfβ1*, *Tgfβ3*, *Cxcl5*, *Tnf*, *Il6*, and *Il1β*: inflammatory mediators; *Ptprc*, *Gfap*: micro- and macroglial activation. Quantitative reverse transcription-polymerase chain reaction data are expressed as fold change versus intact (value 1) ± standard error of the mean (SEM). †$P < 0.05$, ††$P < 0.01$, *vs.* intact; *$P < 0.05$, **$P < 0.01$, ***$P < 0.001$, *vs*. vehicle within the same group; ϕ$P < 0.05$, immunosuppressed vehicle-injected retinas *vs*. non-immunosuppressed; δ$P<0.05$, δδ$P < 0.01$, δδδ$P < 0.001$, immunosuppressed TEG3-injected *vs.* non-immunosuppressed TEG3-injected retinas (non-parametric Mann-Whitney *U* tests). $n = 5$ retinas/group with 3 replicates/plate. IMMUNO: Immunosuppression; ONC: optic nerve crush; RGCs: retinal ganglion cells; TEG3: OEG immortalized clonal cell line; Veh: vehicle.

Microglial activation after transplantation in axotomized retinas differed significantly from that observed after ONC alone (for microglial dynamics after ONC in the rat, see Nadal-Nicolás et al., 2017). This response led us to test the intrinsic effect of TEG3 on intact retinas in both transplantation models. Both TEG3 transplants strongly activated microglial cells and caused RGC death, which was observed at 21 days but not at 7 days after transplantation and was higher in the allogeneic than in the syngeneic mode.

Thus, the late toxic effect of the graft itself on RGCs may have outweighed the neuroprotective properties of allogeneic TEG3, explaining why their neuroprotection on axotomized RGCs did not last 21 days.

The graft toxicity was not additive to ONC, as the number of RGCs in the vehicle and TEG3-axotomized retinas was similar at 21 days. This may indicate differential retina-TEG3 crosstalk depending on host status (intact *versus* injured), as has been described for other cell types transplanted in the same paradigms (Millán-Rivero et al., 2018)

Allogeneic TEG3-induced RGC death in intact retinas depends on microglia and inflammation, as both minocycline and immunosuppression partially rescue RGCs. However, in the syngeneic mode, RGC loss was not rescued by minocycline, indicating that its neurotoxicity is microglia-independent.

These data suggest that TEG3 toxicity has at least two pathways, one allograft-specific dependent on microglia and inflammation and another intrinsic to TEG3 and independent of graft type. It is widely recognized that CNS lacks constitutive expression of MHC II (Hickey and Kimura, 1987; Perry, 1998; Hamo et al., 2007; Romo-González et al., 2012; Kolomeyer and Zarbin, 2014), although activated ameboid microglia express MHC class II molecules (Kreutzberg, 1996; Aloisi et al., 1998; Carson et al., 1998; Ponomarev et al., 2005). We have found that olfactory bulb OEG cells, including primary cultured OEG and TEG3 cell lines, immunostain for MHCII molecules. Additionally, we have assessed that these cells express these molecules in our previous microarray data analysis (Pastrana et al., 2006). Therefore, TEG3 cells may act as antigen-presenting cells and be involved in the MHC class II-mediated extracellular antigen processing and presentation, perhaps triggering the adaptative response of the immune system in response to phagocytosis, and probably causing the activation of T cells in certain physio-pathological conditions (Kuchroo et al., 1995; Ranger et al., 1996; Das et al., 1997; Bettelli et al., 1998). This exciting possibility merits further studies to delve into these mechanisms.

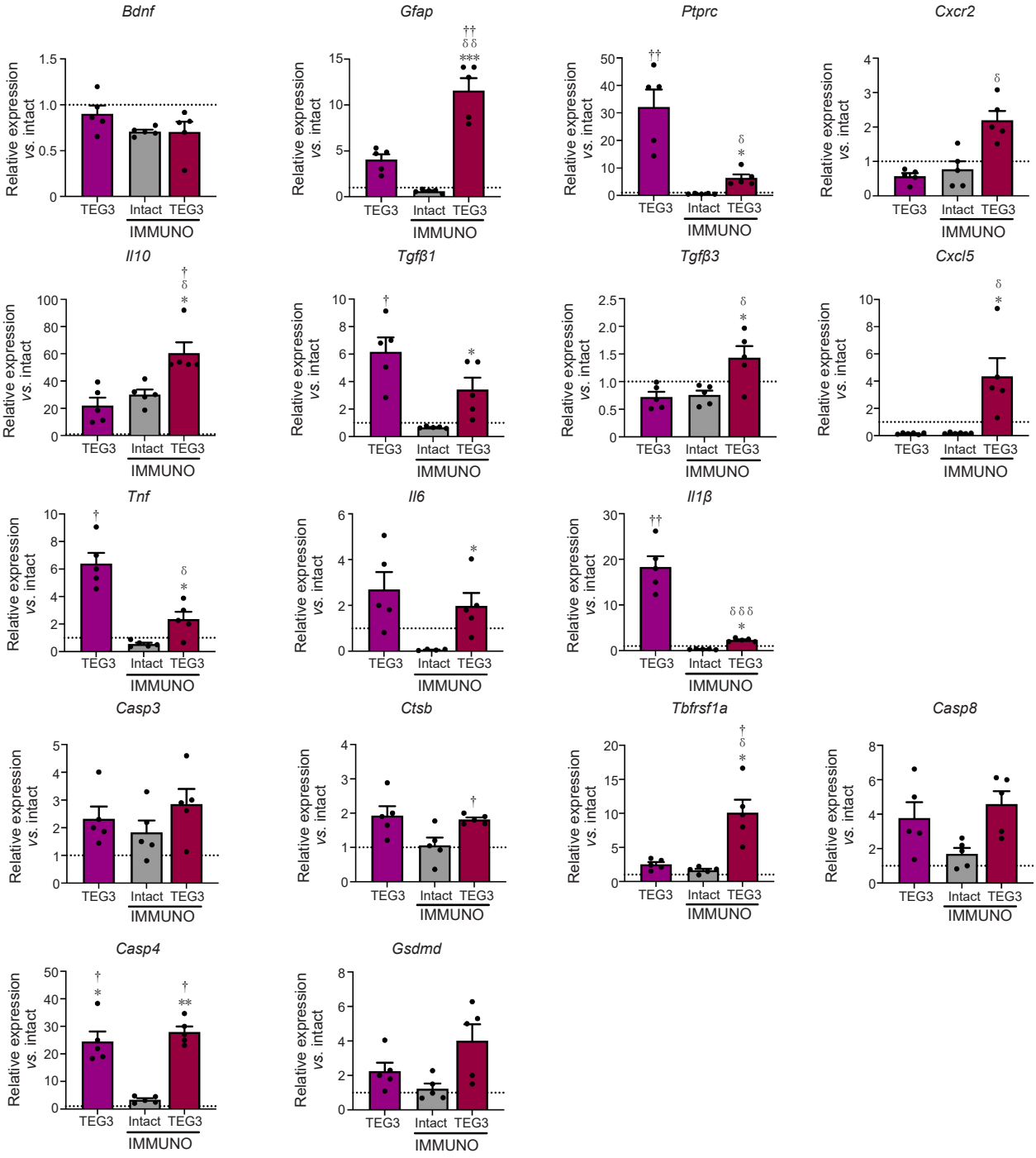

Figure 8 | **Effect of TEG3 transplantation and immunosuppression on gene expression in intact retinas.**
Bar graphs showing gene expression levels 21 days after TEG3 allogeneically transplantated in intact retinas with or without INMUNO compared with intact non-immunosuppressed retinas (value 1, horizontal dashed line). *Bdnf*: Neuroprotective trophic factor; *Cxcr2*, *Il10*, *Tgfβ1*, *Tgfβ3*, *Cxcl5*, *Tnf*, *Il6*, and *Il1β*: inflammatory mediators; *Ptprc*, *Gfap*: micro- and macroglial activation; *Casp3*, *Ctsb*, *Tbfrsf1a*, *Casp8*, *Casp4*, *Gsdmd*: death pathways. Quantitative reverse transcription-polymerase chain reaction data are expressed as fold change *versus* intact (value 1) ± standard error of the mean (SEM). †P < 0.05, ††P < 0.01, *vs.* intact; *P < 0.05, **P < 0.01, ***P < 0.001, *vs*. immunosuppressed intact retinas; δP < 0.05, δδP < 0.01, δδδP < 0.001, *vs*. non-immunosuppressed TEG3-injected retinas (non-parametric Mann–Whitney *U* tests). n = 5 retinas/group with 3 replicates/plate. IMMUNO: Immunosuppression; TEG3: OEG immortalized clonal cell line; Veh: vehicle.

BDNF plays a vital role in microglia inflammatory responses, being a critical regulator of microglial motility (Ding et al., 2020). There is no change in the levels of Bdnf expression in intact retinas *versus* intact + TEG3 allogeneic graft. Despite this, there is a microglial activation 7 days after transplantation, and at 21 days, microglia shows an ameboid shape. This morphotype is more associated with phagocytosis and chemotaxis (Rava et al., 2022; Scipioni et al., 2022; La Torre et al., 2023). Levels of BDNF are also unchanged with immunosuppression in intact retinas with or without TEG3 transplantation. However, in immunosuppressed intact retinas + TEG3 allogeneic graft, microglial cells are less ameboid in comparison with non-immunosuppressed rats. They appear as a mixed population between activated and ameboid. In

this case, the attraction of microglia is lower than in non-immunosuppressed animals. This may account for the decreased neurotoxic effect that we have found.

In intact retinas, the TEG3 allogeneic graft significantly increased the expression of *Casp4*, which is activated in the non-canonical inflammasome pathway of pyroptosis (Cui et al., 2021), and this expression was not altered by immunosuppression. In pyroptosis, *IL1β* is also produced (Cui et al., 2021), which agrees with our qRT-PCR results. In the corresponding paradigm with immunosuppression, Il1β expression is very significantly reduced, in parallel with a decrease in neurotoxicity by TEG3. In amyotrophic lateral sclerosis, inflammation-induced neurotoxicity leads to the activation of microglia and astrocytes to produce IL1β, further leading to motor neuron death (Meissner et al., 2010; Philips and Robberecht, 2011). Therefore, our data suggest that TEG3 toxicity causes pyroptotic RGC death (*Casp4* and *Il1β* upregulation) through microglial activation, being partially controlled by the immunosuppressive treatment (*Il1β* downregulation).

It has been demonstrated that TNF upregulation in microglia has an essential role in the graft-*versus*-host disease of CNS (Mathew et al., 2020). In our models of allogeneic transplantation, *Tnf* is upregulated after TEG3 transplantation, both in intact retinas and after ONC. TNF is the canonical ligand of TNFRS1a. Immunosuppression downregulated *Tnf* expression after TEG3 transplantation, but in intact retinas, it increased that of its receptor *Tnfrs1a*. It is, therefore, possible that lymphotoxin-alpha (LT-α), the other ligand of TNFRS1a (Lindhout et al., 2021), mediates the loss of RGCs that cannot be rescued by minocycline or immunosuppression in TEG3 allogeneic transplants. Thus, RGCs not rescued by immunosuppression may die by extrinsic apoptosis.

In addition to the decrease in the expression of *IL1β*, the upregulation in these retinas of *Il10*, an anti-inflammatory cytokine that damps microglial activation, may contribute to the RGC rescue by immunosuppression after allogeneic TEG3 administration. In fact, in the context of the expression of MHCII molecules by TEG3 and the presence of costimulatory molecules, such as CD86, these cells might stimulate naïve T cells to differentiate into Th2 cells, enhancing, among other things, IL10 production (Kuchroo et al., 1995b; Ranger et al., 1996; Das et al., 1997; Bettelli et al., 1998). Again, these responses merit additional studies.

CXCL5/LPS-induced chemokine (LIX) is a chemokine highly expressed by TEG3, a leukocyte chemoattractant, including macrophages (MohanKumar et al., 2012). Microglia also expresses *Cxcr2*, the CXCL5 receptor (Li et al., 2016). Seven days after ONC, both in TEG3 allogeneic transplantation or vehicle-treated retinas, there is a significant reduction in *Cxcl5* expression in immunosuppressed animals, and neuroprotection by TEG3 was not significantly different from that obtained without immunosuppression. Additionally, *Cxcl5* expression is not significantly different in intact retinas *versus* intact transplanted with TEG3. However, in this model, TEG3 graft + immunosuppression significantly increased *Cxcl5* expression and that of its receptor, *Cxcr2*. This also contrasts with the diminished neurotoxic effect in these TEG3 transplanted immunosuppressed animals, and with their microglial morphotype, less ameboid compared to TEG3 grafted retinas in control animals. This chemokine and its receptor do not seem to have a direct role in the microglial response, at least attracting these cells to the vitreal environment after TEG3 transplantation.

Minocycline alone neuroprotected axotomized RGCs, suggesting that microglial cells do indeed play a role in axotomy-induced RGC death in rats, in contrast to reports in mice (Hilla et al., 2017; Lucas-Ruiz et al., 2019). Systemic immunosuppression also rescued axotomized RGCs better than with allogeneic TEG3. This could be due to the lower expression of *Bdnf* and higher expression of *Tnf* and *Il1β* in TEG3 compared to vehicle-immunosuppressed retinas.

The overexpression of Bdnf explains allogeneic TEG3 neuroprotection of axotomized RGCs. It is independent of inflammation and microglial activation because there are no additive or synergistic effects with immunosuppression or minocycline treatments. Although immunosuppression downregulated *Bdnf* in ONC + TEG3 retinas, it did not impair TEG3 neuroprotection, possibly because it increased *Il10* expression and decreased *Tnf*.

However, this study has several limitations that should be overcome in the future studies. First, we used only females, so results in males may be different. Second, analysis of longer time points would provide valuable information on the persistence of TEG3 neuroprotection on axotomized RGCs. Third, anatomical analyses of the regulated genes shown here would have been useful to identify the retinal cells, whether neurons or glia, involved in the response to TEG3 transplantation.

In conclusion, this study assessed the neuroprotective potential of OEGs and found that although they do have neuroprotective properties, they are also toxic to RGCs. This is the most important and surprising result. When injected intravitreally, other cell types, such as bone marrow-derived mesenchymal stromal cells, induce microglial activation (to a lesser extent than TEG3) and create a pro-inflammatory environment. Still, they do not cause RGC death (Norte-Muñoz et al., 2022). One would have expected better tolerance to OEGs than to BM-MSCs, given that the latter are mesoderm-derived and OEGs neuroectoderm-derived.

Given the massive microglial activation induced by TEG3 transplantation in intact and injured retinas, we expected that microglial inhibition and inflammation dampening would counteract TEG3 toxicity and enhance the neuroprotection caused by allogeneic TEG3. This was not the case; these treatments in intact retinas partially attenuated TEG3 toxicity in allogeneic transplantation, had no effect on syngeneic toxicity, and, after ONC, did not add to the neuroprotection of allogeneic TEG3. Thus, there are intrinsic TEG3 mechanisms that are neurotoxic and neuroprotective, and this fact may also apply to other cell types. On one hand, the neurotoxic effect of TEG3 is due to pyroptosis. On the other hand, the expression of MHCII by TEG3 is a novel and surprising finding. This property and their ability to induce the expression of *Il10* and secrete BDNF may explain some of their neuroprotective

properties. We have also found that immunosuppression has a neuroprotective effect; it would be interesting to investigate the mechanism further and assess its potential and magnitude in this and other models.

The different neuroprotective properties, different toxic effects, and different responses to microglial inhibitory treatments of OEG in the retina depending on the type of transplant highlight the importance of thorough preclinical studies to explore these variables. Our experience with MSCs (Di Pierdomenico et al., 2022; Norte-Muñoz et al., 2022, 2024) and here with OEG leads us to recommend that preclinical work testing the effect of cells used for advanced therapy be performed in intact tissues and at least in the two most commonly used transplantation modalities in the clinic: syngeneic (autologous) and allogeneic, with and without immunosuppression. Testing human cells in rodents is xenotransplantation and requires more rigorous studies and cautious conclusions.

Acknowledgments: *The authors would like to thank Ana Isabel Antón and Beatriz Revilla (Genomics platform, IMIB, Murcia) for their technical assistance with qRT-PCR, Jose Manuel Bernal Garro (Group of Experimental Ophthalmology. UM-IMIB, Murcia) for his help with animal surgery and processing and M. Dolores Morales García (SIdI-UAM Confocal Microscopy Laboratory; Madrid) for her excellent technical assistance in the acquisition of the confocal microscope images. We specially thank Francisco Wandosell (Centro de Biología Molecular "Severo Ochoa" (CSIC-UAM), Universidad Autónoma de Madrid, Madrid, Spain) for his generous gift of the mouse monoclonal antibody against MHCII RT1B, clone OX-6 (Bio-Rad). The graphical abstract was partially created with BioRender.com (agreement number XN2659TDH0) and modified images from Servier Medical Art licensed under CC BY 4.0.*

Author contributions: *Conception, experimental design, data acquisition, interpretation, analysis, and graphics: MNM; data acquisition and analysis: MPL, PSC, DS, JDP, AGO, MP; funding and experimental design: JS; funding and experimental design: conception, funding, experimental design, data interpretation and writing the first draft of the manuscript: MTMF, MAB. All authors revised the manuscript critically for important intellectual content and approved the final version to be published.*

Conflicts of interest: *The authors declare no competing interests.*

Data availability statement: *All relevant data are within the paper and its Additional files.*

Additional file:

Additional Figure 1: *Microglial inhibition with minocycline does not rescue RGCs from syngeneic TEG3 toxicity in intact retinas.*

References

Agudo M, Woodhoo A, Webber D, Mirsky R, Jessen KR, McMahon SB (2008) Schwann cell precursors transplanted into the injured spinal cord multiply, integrate and are permissive for axon growth. Glia 56:1263-1270.

Aloisi F, Ria F, Penna G, Adorini L (1998) Microglia are more efficient than astrocytes in antigen processing and in Th1 but not Th2 cell activation. J Immunol 160:4671-4680.

Assinck P, Duncan GJ, Hilton BJ, Plemel JR, Tetzlaff W (2017) Cell transplantation therapy for spinal cord injury. Nat Neurosci 20:637-647.

Bettelli E, Das MP, Howard ED, Weiner HL, Sobel RA, Kuchroo VK (1998) IL-10 is critical in the regulation of autoimmune encephalomyelitis as demonstrated by studies of IL-10- and IL-4-deficient and transgenic mice. J Immunol 161:3299-3306.

Bradbury EJ, Burnside ER (2019) Moving beyond the glial scar for spinal cord repair. Nat Commun 10:3879.

Bray GM, Villegas-Pérez MP, Vidal-Sanz M, Aguayo AJ (1987) The use of peripheral nerve grafts to enhance neuronal survival, promote growth and permit terminal reconnections in the central nervous system of adult rats. J Exp Biol 132:5-19.

Bunge MB (2016) Efficacy of Schwann cell transplantation for spinal cord repair is improved with combinatorial strategies. J Physiol 594:3533-3538.

Cajal SR, DeFelipe J, Jones EG (1991) Cajal's degeneration and regeneration of the nervous system, history of neuroscience. Oxford: Oxford University Press.

Carson MJ, Reilly CR, Sutcliffe JG, Lo D (1998) Mature microglia resemble immature antigen-presenting cells. Glia 22:72-85.

Charan J, Kantharia ND (2013) How to calculate sample size in animal studies? J Pharmacol Pharmacother 4:303-306.

Cui J, Zhao S, Li Y, Zhang D, Wang B, Xie J, Wang J (2021) Regulated cell death: discovery, features and implications for neurodegenerative diseases. Cell Commun Signal 19:120.

Dai C, Khaw PT, Yin ZQ, Li D, Raisman G, Li Y (2012) Olfactory ensheathing cells rescue optic nerve fibers in a rat glaucoma model. Transl Vis Sci Technol 1:3.

Dai C, Xie J, Dai J, Li D, Khaw PT, Yin Z, Huo S, Collins A, Raisman G, Li Y (2019) Transplantation of cultured olfactory mucosal cells rescues optic nerve axons in a rat glaucoma model. Brain Res 1714:45-51.

Das MP, Nicholson LB, Greer JM, Kuchroo VK (1997) Autopathogenic T helper cell type 1 (Th1) and protective Th2 clones differ in their recognition of the autoantigenic peptide of myelin proteolipid protein. J Exp Med 186:867-876.

Di Pierdomenico J, Scholz R, Valiente-Soriano FJ, Sánchez-Migallón MC, Vidal-Sanz M, Langmann T, Agudo-Barriuso M, García-Ayuso D, Villegas-Pérez MP (2018) Neuroprotective effects of FGF2 and minocycline in two animal models of inherited retinal degeneration. Invest Ophthalmol Vis Sci 59:4392-4403.

Di Pierdomenico J, Gallego-Ortega A, Martínez-Vacas A, García-Bernal D, Vidal-Sanz M, Villegas-Pérez MP, García-Ayuso D (2022) Intravitreal and subretinal syngeneic bone marrow mononuclear stem cell transplantation improves photoreceptor survival but does not ameliorate retinal function in two rat models of retinal degeneration. Acta Ophthalmol 100:e1313-1331.

Ding H, Chen J, Su M, Lin Z, Zhan H, Yang F, Li W, Xie J, Huang Y, Liu X, Liu B, Zhou X (2020) BDNF promotes activation of astrocytes and microglia contributing to neuroinflammation and mechanical allodynia in cyclophosphamide-induced cystitis. J Neuroinflammation 17:19.

García-Escudero V, García-Gómez A, Langa E, Martín-Bermejo MJ, Ramírez-Camacho R, García-Berrocal JR, Moreno-Flores MT, Avila J, Lim F (2012) Patient-derived olfactory mucosa cells but not lung or skin fibroblasts mediate axonal regeneration of retinal ganglion neurons. Neurosci Lett 509:27-32.

Gómez RM, Sánchez MY, Portela-Lomba M, Ghotme K, Barreto GE, Sierra J, Moreno-Flores MT (2018) Cell therapy for spinal cord injury with olfactory ensheathing glia cells (OECs). Glia 66:1267-1301.

González-Riquelme MJ, Galindo-Romero C, Lucas-Ruiz F, Martínez-Carmona M, Rodríguez-Ramírez KT, Cabrera-Maqueda JM, Norte-Muñoz M, Vidal-Sanz M, Agudo-Barriuso M (2021) Axonal injuries cast long shadows: long term glial activation in injured and contralateral retinas after unilateral axotomy. Int J Mol Sci 22:8517.

Hamo L, Stohlman SA, Otto-Duessel M, Bergmann CC (2007) Distinct regulation of MHC molecule expression on astrocytes and microglia during viral encephalomyelitis. Glia 55:1169-1177.

Hickey WF, Kimura H (1987) Graft-vs.-host disease elicits expression of class I and class II histocompatibility antigens and the presence of scattered T lymphocytes in rat central nervous system. Proc Natl Acad Sci U S A 84:2082-2086.

Hilla AM, Diekmann H, Fischer D (2017) Microglia are irrelevant for neuronal degeneration and axon regeneration after acute injury. J Neurosci 37:6113-6124.

Khankan RR, Griffis KG, Haggerty-Skeans JR, Zhong H, Roy RR, Edgerton VR, Phelps PE (2016) Olfactory ensheathing cell transplantation after a complete spinal cord transection mediates neuroprotective and immunomodulatory mechanisms to facilitate regeneration. J Neurosci 36:6269-6286.

Klinker MW, Marklein RA, Lo Surdo JL, Wei CH, Bauer SR (2017) Morphological features of IFN-γ-stimulated mesenchymal stromal cells predict overall immunosuppressive capacity. Proc Natl Acad Sci U S A 114:E2598-2607.

Kobayashi K, Imagama S, Ohgomori T, Hirano K, Uchimura K, Sakamoto K, Hirakawa A, Takeuchi H, Suzumura A, Ishiguro N, Kadomatsu K (2013) Minocycline selectively inhibits M1 polarization of microglia. Cell Death Dis 4:e525.

Kolomeyer AM, Zarbin MA (2014) Trophic factors in the pathogenesis and therapy for retinal degenerative diseases. Surv Ophthalmol 59:134-165.
Kreutzberg GW (1996) Microglia: a sensor for pathological events in the CNS. Trends Neurosci 19:312-318.
Kuchroo VK, Das MP, Brown JA, Ranger AM, Zamvil SS, Sobel RA, Weiner HL, Nabavi N, Glimcher LH (1995) B7-1 and B7-2 costimulatory molecules activate differentially the Th1/Th2 developmental pathways: application to autoimmune disease therapy. Cell 80:707-718.
La Torre ME, Cianciulli A, Monda V, Monda M, Filannino FM, Antonucci L, Valenzano A, Cibelli G, Porro C, Messina G, Panaro MA, Messina A, Polito R (2023) α-Tocopherol protects lipopolysaccharide-activated BV2 microglia. Molecules 28:3340.
Lambuk L, Mohd Lazaldin MA, Ahmad S, Iezhitsa I, Agarwal R, Uskoković V, Mohamud R (2022) Brain-derived neurotrophic factor-mediated neuroprotection in glaucoma: a review of current state of the art. Front Pharmacol 13:875662.
Li Y, Sauvé Y, Li D, Lund RD, Raisman G (2003) Transplanted olfactory ensheathing cells promote regeneration of cut adult rat optic nerve axons. J Neurosci 23:7783-7788.
Li Y, Du XL, He BP (2016) Lipopolysaccharide Upregulates the Expression of CINC-3 and LIX in Primary NG2 Cells. Neurochem Res 41:1448-1457.
Lim F, Martín-Bermejo MJ, García-Escudero V, Gallego-Hernández MT, García-Gómez A, Rábano A, Díaz-Nido J, Avila J, Moreno-Flores MT (2010) Reversibly immortalized human olfactory ensheathing glia from an elderly donor maintain neuroregenerative capacity. Glia 58:546-558.
Lindhout IA, Murray TE, Richards CM, Klegeris A (2021) Potential neurotoxic activity of diverse molecules released by microglia. Neurochem Int 148:105117.
Lindsay SL, Toft A, Griffin J, M M Emraja A, Barnett SC, Riddell JS (2017) Human olfactory mesenchymal stromal cell transplants promote remyelination and earlier improvement in gait co-ordination after spinal cord injury. Glia 65:639-656.
Livak KJ, Schmittgen TD (2001) Analysis of relative gene expression data using real-time quantitative PCR and the 2(-Delta Delta C(T)) method. Methods 25:402-408.
Lucas-Ruiz F, Galindo-Romero C, Rodríguez-Ramírez KT, Vidal-Sanz M, Agudo-Barriuso M (2019) Neuronal death in the contralateral un-injured retina after unilateral axotomy: role of microglial cells. Int J Mol Sci 20:5733.
Martin KR, Quigley HA (2004) Gene therapy for optic nerve disease. Eye (Lond) 18:1049-1055.
Mathew NR, et al. (2020) Graft-versus-host disease of the CNS is mediated by TNF upregulation in microglia. J Clin Invest 130:1315-1329.
Meissner F, Molawi K, Zychlinsky A (2010) Mutant superoxide dismutase 1-induced IL-1beta accelerates ALS pathogenesis. Proc Natl Acad Sci U S A 107:13046-13050.
Millán-Rivero JE, Nadal-Nicolás FM, García-Bernal D, Sobrado-Calvo P, Blanquer M, Moraleda JM, Vidal-Sanz M, Agudo-Barriuso M (2018) Human Wharton's jelly mesenchymal stem cells protect axotomized rat retinal ganglion cells via secretion of anti-inflammatory and neurotrophic factors. Sci Rep 8:16299.
MohanKumar K, Kaza N, Jagadeeswaran R, Garzon SA, Bansal A, Kurundkar AR, Namachivayam K, Remon JI, Bandepalli CR, Feng X, Weitkamp JH, Maheshwari A (2012) Gut mucosal injury in neonates is marked by macrophage infiltration in contrast to pleomorphic infiltrates in adult: evidence from an animal model. Am J Physiol Gastrointest Liver Physiol 303:G93-102.
Moreno-Flores MT, Lim F, Martín-Bermejo MJ, Díaz-Nido J, Avila J, Wandosell F (2003) Immortalized olfactory ensheathing glia promote axonal regeneration of rat retinal ganglion neurons. J Neurochem 85:861-871.
Moreno-Flores MT, Bradbury EJ, Martín-Bermejo MJ, Agudo M, Lim F, Pastrana E, Avila J, Díaz-Nido J, McMahon SB, Wandosell F (2006) A clonal cell line from immortalized olfactory ensheathing glia promotes functional recovery in the injured spinal cord. Mol Ther 13:598-608.
Nadal-Nicolás FM, Jiménez-López M, Sobrado-Calvo P, Nieto-López L, Cánovas-Martínez I, Salinas-Navarro M, Vidal-Sanz M, Agudo M (2009) Brn3a as a marker of retinal ganglion cells: qualitative and quantitative time course studies in naive and optic nerve-injured retinas. Invest Ophthalmol Vis Sci 50:3860-3868.
Nadal-Nicolás FM, Sobrado-Calvo P, Jiménez-López M, Vidal-Sanz M, Agudo-Barriuso M (2015) Long-term effect of optic nerve axotomy on the retinal ganglion cell layer. Invest Ophthalmol Vis Sci 56:6095-6112.
Nadal-Nicolás FM, Jiménez-López M, Salinas-Navarro M, Sobrado-Calvo P, Vidal-Sanz M, Agudo-Barriuso M (2017) Microglial dynamics after axotomy-induced retinal ganglion cell death. J Neuroinflammation 14:218.
Norte-Muñoz M, Lucas-Ruiz F, Gallego-Ortega A, García-Bernal D, Valiente-Soriano FJ, de la Villa P, Vidal-Sanz M, Agudo-Barriuso M (2021) Neuroprotection and axonal regeneration induced by bone marrow mesenchymal stromal cells depend on the type of transplant. Front Cell Dev Biol 9:772223.
Norte-Muñoz M, Gallego-Ortega A, Lucas-Ruiz F, González-Riquelme MJ, Changa-Espinoza YI, Galindo-Romero C, Ponsaerts P, Vidal-Sanz M, García-Bernal D, Agudo-Barriuso M (2022) Immune recognition of syngeneic, allogeneic and xenogeneic stromal cell transplants in healthy retinas. Stem Cell Res Ther 13:430.
Norte-Muñoz M, García-Bernal D, García-Ayuso D, Vidal-Sanz M, Agudo-Barriuso M (2024) Interplay between mesenchymal stromal cells and the immune system after transplantation: implications for advanced cell therapy in the retina. Neural Regen Res 19:542-547.
Okano H (2002) Stem cell biology of the central nervous system. J Neurosci Res 69:698-707.
Parrilla-Reverter G, Agudo M, Sobrado-Calvo P, Salinas-Navarro M, Villegas-Pérez MP, Vidal-Sanz M (2009) Effects of different neurotrophic factors on the survival of retinal ganglion cells after a complete intraorbital nerve crush injury: a quantitative in vivo study. Exp Eye Res 89:32-41.
Pastrana E, Moreno-Flores MT, Gurzov EN, Avila J, Wandosell F, Diaz-Nido J (2006) Genes associated with adult axon regeneration promoted by olfactory ensheathing cells: a new role for matrix metalloproteinase 2. J Neurosci 26:5347-5359.
Pastrana E, Moreno-Flores MT, Avila J, Wandosell F, Minichiello L, Diaz-Nido J (2007) BDNF production by olfactory ensheathing cells contributes to axonal regeneration of cultured adult CNS neurons. Neurochem Int 50:491-498.
Peinado-Ramón P, Salvador M, Villegas-Pérez MP, Vidal-Sanz M (1996) Effects of axotomy and intraocular administration of NT-4, NT-3, and brain-derived neurotrophic factor on the survival of adult rat retinal ganglion cells. A quantitative in vivo study. Invest Ophthalmol Vis Sci 37:489-500.
Percie du Sert N, et al. (2020) The ARRIVE guidelines 2.0: Updated guidelines for reporting animal research. PLoS Biol 18:e3000410.
Perry VH (1998) A revised view of the central nervous system microenvironment and major histocompatibility complex class II antigen presentation. J Neuroimmunol 90:113-121.
Philips T, Robberecht W (2011) Neuroinflammation in amyotrophic lateral sclerosis: role of glial activation in motor neuron disease. Lancet Neurol 10:253-263.
Ponomarev ED, Shriver LP, Maresz K, Dittel BN (2005) Microglial cell activation and proliferation precedes the onset of CNS autoimmunity. J Neurosci Res 81:374-389.
Portela-Lomba M, Simón D, Russo C, Sierra J, Moreno-Flores MT (2020) Coculture of axotomized rat retinal ganglion neurons with olfactory ensheathing glia, as an in vitro model of adult axonal regeneration. J Vis Exp doi: 10.3791/61863.
Ranger AM, Das MP, Kuchroo VK, Glimcher LH (1996) B7-2 (CD86) is essential for the development of IL-4-producing T cells. Int Immunol 8:1549-1560.
Rava A, La Rosa P, Palladino G, Dragotto J, Totaro A, Tiberi J, Canterini S, Oddi S, Fiorenza MT (2022) The appearance of phagocytic microglia in the postnatal brain of Niemann Pick type C mice is developmentally regulated and underscores shortfalls in fine odor discrimination. J Cell Physiol 237:4563-4579.
Roet KC, Verhaagen J (2014) Understanding the neural repair-promoting properties of olfactory ensheathing cells. Exp Neurol 261:594-609.
Romo-González T, Chavarría A, Pérez-H J (2012) Central nervous system: a modified immune surveillance circuit? Brain Behav Immun 26:823-829.
Sánchez-Migallón MC, Nadal-Nicolás FM, Jiménez-López M, Sobrado-Calvo P, Vidal-Sanz M, Agudo-Barriuso M (2011) Brain derived neurotrophic factor maintains Brn3a expression in axotomized rat retinal ganglion cells. Exp Eye Res 92:260-267.
Scipioni L, Ciaramellano F, Carnicelli V, Leuti A, Lizzi AR, De Dominicis N, Oddi S, Maccarrone M (2022) Microglial endocannabinoid signalling in AD. Cells 11:1237.
Vidal-Sanz M, Avilés-Trigueros M, Whiteley SJ, Sauvé Y, Lund RD (2002) Reinnervation of the pretectum in adult rats by regenerated retinal ganglion cell axons: anatomical and functional studies. Prog Brain Res 137:443-452.
Vidal-Sanz M, Galindo-Romero C, Valiente-Soriano FJ, Nadal-Nicolás FM, Ortin-Martinez A, Rovere G, Salinas-Navarro M, Lucas-Ruiz F, Sanchez-Migallon MC, Sobrado-Calvo P, Aviles-Trigueros M, Villegas-Pérez MP, Agudo-Barriuso M (2017) Shared and differential retinal responses against optic nerve injury and ocular hypertension. Front Neurosci 11:235.

C-Editor: Zhao M; S-Editor: Li CH; L-Editors: Li CH, Song LP; T-Editor: Jia Y